Experimental Eye Research 171 (2018) 37–47

Contents lists available at ScienceDirect

Experimental Eye Research

journal homepage: www.elsevier.com/locate/yexer

Diesel exhaust particles (DEP) induce an early redox imbalance followed by an IL-6 mediated inflammatory response on human conjunctival epithelial cells

Romina M. Lasagni Vitar[a,b,*], Julia Tau[c], Natasha S. Janezic[a], Agustina I. Tesone[c], Ailen G. Hvozda Arana[a], Claudia G. Reides[a,b], Alejandro Berra[c], Sandra M. Ferreira[a,b], Susana F. Llesuy[a,b]

[a] University of Buenos Aires, Faculty of Pharmacy and Biochemistry, Analytical Chemistry and Phisicochemistry Department, General and Inorganic Chemistry Division, Buenos Aires, Argentina
[b] CONICET- University of Buenos Aires, Instituto de Bioquímica y Medicina Molecular (IBIMOL), Buenos Aires, Argentina
[c] University of Buenos Aires, Faculty of Medicine, Pathology Department, Ocular Investigation Laboratory, Buenos Aires, Argentina

ARTICLE INFO

Keywords:
Conjunctiva
Oxidative stress
Antioxidants
Inflammation
Diesel exhaust particles

ABSTRACT

The aim of this study was to evaluate the time course of oxidative stress markers and inflammatory mediators in human conjunctival epithelial cells (IOBA-NHC) exposed to diesel exhaust particles (DEP) for 1, 3, and 24 h.

Reactive oxygen species (ROS) production, lipid and protein oxidation, Nrf2 pathway activation, enzymatic antioxidants, glutathione (GSH) levels and synthesis, as well as cytokine release and cell proliferation were analyzed.

Cells exposed to DEP showed an increase in ROS at all time points. The induction of NADPH oxidase-4 appeared later than mitochondrial superoxide anion production, when the cell also underwent a proinflammatory response mediated by IL-6. DEP exposure triggered the activation of Nrf2 in IOBA-NHC, as a strategy for increasing cellular antioxidant capacity. Antioxidant enzyme activities were significantly increased at early stages except for glutathione reductase (GR) that showed a significant decrease after a 3-h-incubation. GSH levels were found increased after 1 and 3 h of incubation with DEP, despite the increase in its consumption by the antioxidant enzymes as it works as a cofactor. GSH recycling and the *de novo* synthesis were responsible for the maintenance of its content at these time points, respectively. After 24 h, the decrease in GR and glutamate cysteine ligase as wells as the enhanced activity of glutathione peroxidase and glutathione S-transferase produced a depletion in the GSH pool. Lipid-peroxidation was found increased in cells exposed to DEP after 1-h-incubation, whereas protein oxidation was found increased in cells exposed to DEP after a 3-h-incubation that persisted after a longer exposure. Furthermore, DEP lead IOBA-NHC cells to hyperplasia after 1 and 3 h of incubation, but a decrease in cell proliferation was found after longer exposure.

ROS production seems to be an earlier event triggered by DEP on IOBA-NHC, comparing to the proinflammatory response mediated by IL-6. Despite the fact that under short periods of exposure to DEP lipids and then proteins are targets of oxidative damage, the viability of the cells is not affected at early stages, since cell hyperplasia was detected as compensatory mechanism. Although after 24 h Nrf2 pathway is still enhanced, the epithelial cell capacity to maintain redox balance is exceeded. The antioxidant enzymes activation and the depleted GSH pool are not capable of counteracting the increased ROS production, leading to oxidative damage.

1. Introduction

Epidemiological evidence demonstrates that in our days air pollution is the largest environmental risk factor, leading to increased mortality and morbidity (World Health Organization, 2016). Particulate matter (PM) is a key ingredient of polluted air and the main responsible for the health effects due to air pollution (Nel, 2005). Its composition comprises a large number of chemical constituents that generates health effects, ranging from eye irritation to death (Lu, 2014a,b).

The ocular surface is now considered as an important target of air

* Corresponding author. Cátedra de Química General e Inorgánica, Facultad de Farmacia y Bioquímica, Universidad de Buenos Aires, Junín 954, C1113AAD, Buenos Aires, Argentina.
E-mail address: rlasagni@ffyb.uba.ar (R.M. Lasagni Vitar).

https://doi.org/10.1016/j.exer.2018.03.005
Received 29 December 2017; Received in revised form 23 February 2018; Accepted 6 March 2018
Available online 07 March 2018
0014-4835/

pollution effects because it is almost constantly exposed to air pollutants, separated from the environment only by the tear film. Moreover, several studies have demonstrated that people from urban centers present eye discomfort symptoms, as well as aggravation of pre-existing ocular diseases (Berra et al., 2015; Fu et al., 2017; Hwang et al., 2016; Nucci et al., 2017; Torricelli et al., 2014). Conjunctiva epithelia capacity to respond quickly to infections and trauma is important to protect the eye from the environment, but also makes it particularly sensitive to mechanical, toxic and immunological injuries (Tsubota et al., 2002).

The occurrence of oxidative stress as well as inflammatory processes have been identified by both *in vivo* and *in vitro* studies as one of the mechanisms by which air pollution particles cause adverse biological effects (Lasagni Vitar et al., 2015; Li et al., 2008; Magnani et al., 2016; Marchini et al., 2014; Tau et al., 2013). Reactive oxygen species (ROS) are produced by several cellular sources. Mitochondria and NADPH oxidases have been demonstrated to play a central role in the development of cellular response to environmental stressors in tissues such as lung and skin (Lee et al., 2016; Lee and Yang, 2012; Magnani et al., 2011; Xia et al., 2007). However, the involvement of both Mitochondria and NADPH oxidases in the conjunctival response to particulate matter has not yet been reported.

It is known that a well-constituted antioxidant system is needed to respond to oxidative insults and to maintain the redox homeostasis. However, there are few studies about the antioxidant present on the ocular surface, especially on the conjunctiva (Chen et al., 2009; Lasagni Vitar et al., 2015; Nezzar et al., 2017). The nuclear factor-erythroid 2-related factor-2 (Nrf2) is crucial in the modulation of cellular adaptive response to oxidative stress. Nrf2 transcriptionally up regulates antioxidant genes, including phase II detoxifying enzymes and antioxidants (Rubio et al., 2010). Additionally, the homeostasis of glutathione (GSH) levels, the most abundant cellular non-protein thiol, together with its oxidized form (GSSG) help to maintain the cellular redox status. Moreover, several studies have provided evidence that changes in GSH homeostasis is associated with various human diseases affecting the ocular surface epithelia (Chen et al., 2009).

Although our previous findings demonstrate that diesel exhaust particles (DEP) trigger a toxic response mediated by both oxidative stress and inflammatory mediators, the time course of these events is still unknown. The understanding of the toxic mechanism triggered by air pollutants on urban population eyes is necessary since ocular surface response is determinant to ensure eye survival. Therefore, the aim of the present study was to evaluate the time course of oxidative stress markers and inflammatory mediators in human conjunctival epithelial cells (IOBA-NHC) exposed to diesel exhaust particles (DEP) for 1, 3, and 24 h, analyzing the mechanism underlying the toxic effects.

2. Materials and methods

2.1. Cell culture

The normal human conjunctival epithelium cell line (IOBA-NHC) was kindly provided by Dr. Yolanda Diebold (University Institute of Applied Ophthalmobiology, University of Valladolid, Valladolid, Spain) (Diebold et al., 2003). IOBA-NHC were grown in DMEM-F12 supplemented with 10% fetal bovine serum, 2 ng/mL EGF, 5 μg/mL hydrocortisone, 1 μg/mL bovine pancreas insulin, 50 U/mL penicillin, 50 μg/mL streptomycin, and 2 mg/mL amphotericin B in a humid atmosphere of 37 °C with 5% CO_2.

2.2. Diesel exhaust particles (DEP)

DEP from diesel motor combustion were kindly provided by Dr. Paulo H. Saldiva (Laboratório de Poluição Atmosférica Experimental, Faculdade de Medicina, Universidade de São Paulo, São Paulo, Brazil). A particle trap device was adapted to the exhaust pipe of a bus from the public transportation fleet, equipped with a Mercedes Benz MB1620, 210-hp engine, without electronic control of fuel injection, running with diesel containing 500 ppm sulfur. DEP are composed of a carbonaceous core with adsorbed organic compounds, including polycyclic aromatic hydrocarbons (PAHs), and trace of inorganic compounds (Laks et al., 2008). A DEP 100 μg/mL suspension was made by weighing DEP, adding culture medium and sonicating in an ultrasonic bath (Ultrasonic Cleaner; Testlab, Bernal Oeste, Buenos Aires, Argentina) for 30 min.

2.3. IOBA-NHC incubation with DEP

IOBA-NHC cell monolayers (80–100% confluent) were incubated with DEP at 100 μg/mL (DEP 100 group) or with culture medium (control group) for 1, 3, and 24 h. Cell monolayers were washed twice with phosphate-buffered saline (PBS) 1X, pH = 7.40. Cells were removed with 0.25% trypsin-EDTA to perform the assays (Tau et al., 2013).

2.4. Measurement of intracellular ROS generation and sources

2.4.1. Total levels of prooxidant species

Cells (2.5×10^5 cells/mL) were incubated with 5 μM 2′,7′-dichlorofluorescein diacetate (DCF-DA). After a 30 min incubation in the dark at 37 °C, the samples were analyzed by flow cytometry, and 50,000 events per sample were acquired (Partec PAS-III flow cytometer (Partec GmbH, Münster, Germany) equipped with a 488 nm argon laser). The cell population was gated based on light scattering properties. DCF signal was analyzed in the FL-1 channel with FlowJo software (TreeStar), and quantified as median fluorescence intensities (MFI) (Lasagni Vitar et al., 2015). The results were expressed as percentage of increase over control cells.

2.4.2. NADPH oxidase-4 (NOX4) expression

Cell lysates were obtained scraping off the monolayers from the culture plate with lysis buffer (50 mM Tris HCl, 150 mM NaCl, 1 mM protease inhibitor (Sigma), 2 mM EDTA, 1% Triton X-100), then sonicated in cold water for 10 min and centrifuged at 800 g for 10 min. Proteins in supernatants were determined by Lowry's method. A sample of 30 μg of proteins was resolved on 10% acrylamide SDS-PAGE gels. Proteins were transferred to PVDF membranes and blocked for 1 h in 5% nonfat dry milk in PBS with 13% NaN_3 and hybridized overnight with anti-NOX4 (1:800; sc-30141, Santa Cruz Biotechnology) or anti-actin (CP01, Calbiochem). Membranes were washed three times in PBS, and secondary detection was performed using HRP-conjugated anti-rabbit antibody (ab 6721, Abcam) at a dilution of 1:5000. Membranes were washed three times, and chemiluminescent detection was performed using ECL (Thermo Scientific). Bands were quantified using ImageJ program (1.50i, Wayne Rasband, National Institutes of Health, USA).

2.4.3. Inner mitochondrial membrane potential ($\Delta\Psi_m$) and superoxide anion production

The potentiometric cationic probe 3,3′-dihexyloxacarbocyanine iodide ($DiOC_6$) and MitoSOX probe were used for the determination by flow cytometry of inner mitochondrial membrane potential and mitochondrial superoxide anion production, respectively. A sample of 1×10^5 IOBA-NHC cells were incubated with $DiOC_6$ (30 nM) or MitoSOX (5 μM) in PBS. The data was collected by FACSCalibur; BD Biosciences, argon laser 488 nm. Samples were gated based on light-scattering properties and 30,000 events per sample were collected. $DiOC_6$ and MitoSOX signals were analyzed in the FL-1 and FL-3 channels, respectively, with FlowJo software (TreeStar), and quantified as median fluorescence intensities (MFI). Results are expressed as percentage of positive cells ($DIOC_6^+$ or $MitoSOX^+$).

2.5. Oxidative damage to macromolecules

2.5.1. Lipid oxidation

Lipid damage was determined as thiobarbituric acid reactive substances (TBARS), by a fluorometric assay (Yagi, 1976), using a Perkin Elmer LS 55 Fluorescence Spectrometer (Perkin Elmer, Waltham, MA, US) at 515 nm (excitation) and 553 nm (emission). Briefly, whole lysate samples (100 μL) were incubated with 200 μL of 0.1 N HCl, 30 μL of 10% w/v phosphotungstic acid, and 100 μL of 0.7% w/v 2- thiobarbituric acid (TBA) in a dry bath. After 60 min, TBARS were extracted in 500 μL of n-butanol and centrifuged at 1000 g for 10 min. A calibration curve was performed using 1,1,3,3-tetramethoxypropane (MDA). Results were expressed as nmol MDA/mg protein.

2.5.2. Protein oxidation

Carbonyl groups from oxidized proteins were detected with 10 mM 2,4-dinitrophenylhydrazine (DNPH). The formation of a stable 2,4-dinitrophenylhydrazone product (DNP) that was soluble in 6 M guanidine was measured at 370 nm (Levine et al., 1990). Results were expressed as nmol/mg protein.

2.6. Nuclear factor-erythroid 2-related factor-2 (Nrf2) immunofluorescence

Cells were plated in a 24-well plate where 12 mm diameter coverslips were previously adhered. After the incubation with DEP, cells were fixed using 4% paraformaldehyde and permeabilized with 0.2% Triton X-100. Cells were blocked in 1% BSA and then, incubated with Nrf2 antibody (1:100; sc-13032, Santa Cruz Biotechnology) overnight in wet-chamber at 4 °C. After PBS 1X washes, a FITC- conjugated secondary antibody (1:200, 31635, Pierce) was used. Nuclei were counter-stained with 0.1 μg/mL DAPI. A mix of glycerol:PBS (1:9) was used to mount coverslip. Samples were visualized using a NIKON Eclipse Ti-E PFS fluorescence microscope, images were captured by ANDOR Neo 5.5 sCMOS camera and analyzed with Image J software. The results were expressed as percentage of cells with Nrf2 nuclear translocation ($Nrf2^+$ cells).

2.7. Activity of antioxidant enzymes defenses and enzymes related to the regulation of the redox status

All enzymatic measurements were performed by a spectrophotometric assay using a Hitachi U-2000 Spectrophotometer (Hitachi Ltd. Chiyoda, Tokyo, Japan).

2.7.1. Superoxide dismutase (SOD)

The reaction medium consisting in 1 mM epinephrine and 50 mM glycine buffer (pH = 10.50). The addition of increasing amounts of cells lysate in the mixture lead to the inhibition of adrenochrome formation rate at 37 °C at 480 nm. Enzymatic activity was expressed as USOD/mg protein. One SOD unit was defined as the volume of sample which inhibit adrenochrome formation rate by 50% (Misra and Fridovich, 1972).

2.7.2. Glutathione peroxidase (GPx)

Cell lysate (20 μL) was mixed in the reaction medium consisted of 100 mM phosphate buffer (pH = 7.50) in presence of 10 μM reduced glutathione, 6 U/ mL glutathione reductase and 10 mM *tert*-butyl hydroperoxide. The activity was determined by following at 340 nm the oxidation of reduced nicotinamide adenine dinucleotide phosphate (NADPH) (Flohé and Günzler, 1984). Results were expressed as μmol/mg protein.min.

2.7.3. Glutathione S-transferase (GST)

In the presence of glutathione, 1 chloro - 2,4 dinitrobenzene (CDNB) forms GS-dinitrobenzene (GS-DNB) that absorbs at 340 nm. The reaction was catalyzed by GST provided by 50 μL of the cell lysate. Briefly, cells lysate was mixed in the reaction medium consisted of phosphate buffer (pH = 6.50), 10 mM glutathione (GSH) and 20 mM CDNB. One GST unit was defined as the amount of enzyme that catalyzes the formation of 1 μmol GS-DNB per minute at 30 °C. Results were expressed as mUGST/mg protein (Habig et al., 1974).

2.7.4. Glutathione reductase (GR)

Cells lysate (50 μL) was mixed in the reaction medium consisted of 100 mM Tris 10 mM EDTA buffer (pH = 8.00), 25 mM oxidized glutathione (GSSG) and 10 mM NADPH. Glutathione reductase activity was determined by following at 340 nm the oxidation of reduced nicotinamide adenine dinucleotide phosphate (NADPH). Results were expressed as μmol/min. mg protein (Racker, 1955).

2.7.5. Thioredoxin reductase (TrxR)

Thioredoxin reductase activity was evaluated spectrophotometrically at 412 nm. Briefly, cells lysate (20 μL) was mixed in the reaction medium comprised of 100 mM phosphate buffer (pH = 7.00), 25 mg/mL DTNB, 20 mg/mL albumin, 0.2 M EDTA and 40 mg/mL NADPH. Results were expressed as mmol/min. mg protein (Holmgren and Björnstedt, 1995).

2.7.6. Glucose 6P-dehidrogenase (G6PDH)

Glucose 6P-dehidrogenase activity was determined by following NADPH reduction at 340 nm. Briefly, cells lysate (20 μL) was mixed in the reaction medium consisted of 85 mM Tris/8.5 mM $MgCl_2$ buffer (pH = 7.50), 20 mM glucose 6P and 10 mM NADP+. Results were expressed as U/min mg of protein. One G6PDH unit was defined as the amount of enzyme that catalyzes the transformation of 1 mmol of substrate per minute, per mg of protein (Leong and Clark, 1984).

2.8. Glutathione synthesis

2.8.1. Reduced (GSH) glutathione levels

Cells lysate samples (100 μL) were mixed with 1 M $HClO_4$-2 mM EDTA (1:1) and centrifuged at 20,000 g for 20 min at 4 °C. Supernatants were filtered through 0.22 μm cellulose acetate membranes (Corning Inc. NY, US) and frozen at −80 °C until use. HPLC analysis was performed in a Perkin Elmer LC 250 liquid chromatography (Perkin Elmer, Waltham, MA, US), equipped with a Perkin Elmer LC ISS 200 advanced sample processor and a Coulochem II (ESA, Bedford, MA, US) electrochemical detector. A Supelcosil LC-18 (250 × 4.6 mm ID, 5 μm particle size) column protected by a Supelguard (20 × 4.6 mm ID) precolumn (Supelco, Bellfonte, PA, US) was used for sample separation. GSH was eluted at a flow rate of 1.2 mL/min with 20 mM sodium phosphate (pH = 2.70), and electrochemically detected at an applied oxidation potential of +0.800 V. A calibration curve with GSH standard was performed. Results were expressed as nmol/1×10^6 cells (Lasagni Vitar et al., 2015).

2.8.2. Glutamate cysteine ligase (GCL) expression

Samples were obtained as previously described (Section 2.4.2). A sample of 30 μg of proteins was resolved on 10% acrylamide SDS-PAGE gels. Proteins were transferred to PVDF membranes and blocked for 1 h in 5% nonfat dry milk in PBS with 13% NaN_3 and hybridized overnight with anti-GCL (1:400; sc-390811, Santa Cruz Biotechnology) or anti-actin (CP01, Calbiochem). Membranes were washed three times in PBS, and secondary detection was performed using HRP-conjugated anti-mouse antibody (Cappel) at a dilution of 1:5000. Membranes were washed three times, and chemiluminescent detection was performed using ECL (Thermo Scientific). Bands were quantified using ImageJ program (1.50i, Wayne Rasband, National Institutes of Health, USA).

2.8.3. Aminoacid analysis

Aminoacid analysis was carried out using an Ultra Performance Liquid Chromatographic system combined with a Waters Acquity binary solvent manager (BSM), an Acquity I-Class sample manager (SM), a column heater, an eλ photodiode array detector (PDA), and a Waters MassTrak™ Amino Acid Analysis Kit. The kit utilizes pre-column derivatization of aminoacids with 6-aminoquinolyl-N-hydroxysuccinimdyl carbamate,

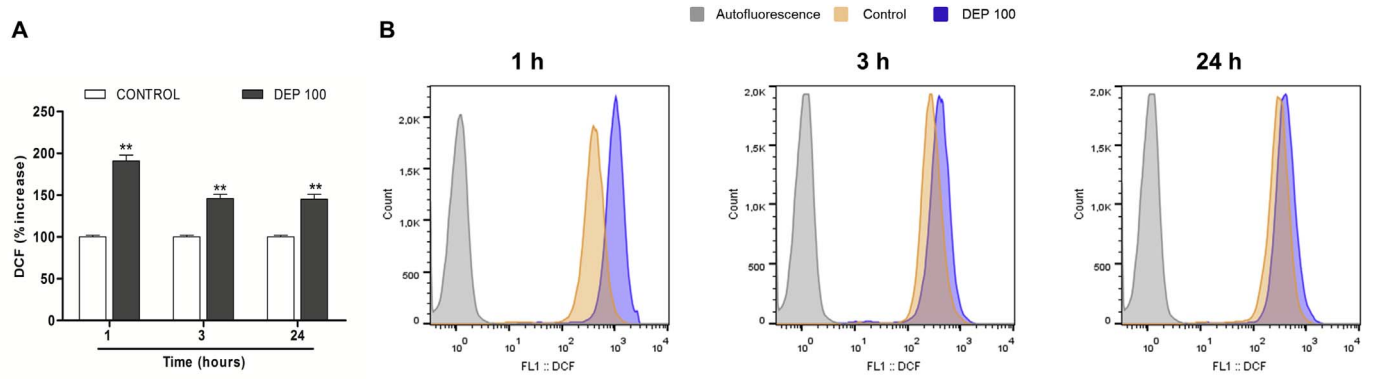

Fig. 1. Total levels of prooxidant species. A- DCF fluorescence quantification of gated cells was performed as MFI after 1, 3 and, 24 h of incubation with DEP. Results are expressed as fold of increase. Results are expressed as mean ± SEM. $^{**}p < 0.01$ B- Representative overlaid histograms of DCF fluorescence of control and DEP100 group.

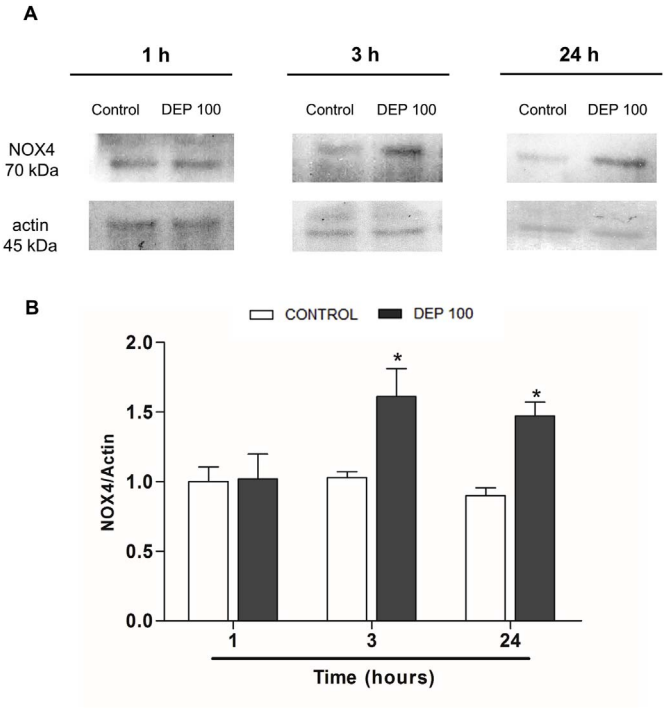

Fig. 2. Expression of NOX4 was determined by Western blotting. A- A representative blot is shown. Bands of approximately 70 kDa and 45 kDa correspond to NOX4 and actin, respectively. B- Bars represent the relative protein level calculated by the ratio of NOX4/Actin. Results are expressed as mean ± SEM. $^{*}p < 0.05$.

followed by reversed-phase UPLC on a C18 column (1.7 µm; 2.1 × 150 mm) and UV detection at 260 nm. A sample of 200 µL was deproteinized with an equal volume of 10% v/v sulfosalicylic acid containing the internal standard Norvaline at a final concentration of 250 µmol/L. Samples were centrifuged at 12,000 g for 5 min and the supernatant removed for derivatization according to the manufacturer's instructions. Derivatized products were transferred to a sample vial for analysis (1 µL injection).

2.9. Proinflammatory cytokine determination

Cytokine release was evaluated in culture supernatants. In order to eliminate the particles, the media were centrifuged at 10,000 g for 10 min at 4 °C. Particle-free supernatants were used to determine the secretion of TNF-α, IL-1β, IL-6, and IL-8 using ELISA kits (BD Biosciences) following the manufacturer's technical specifications.

2.10. MTT assay

IOBA-NHC cells were plated at 3×10^4 cells per well in a 24-well tissue culture plate and grown for 24 h prior to treatment. After the incubation time with DEP, supernatants were removed, and each well was washed twice with 1X PBS, pH = 7.40. Culture medium with 0.4 mg/mL MTT (3-(4,5-Dimethylthiazol-2-yl) −2,5-Diphenyltetrazolium Bromide, Sigma, Saint Louis, USA) was added to each well (final volume = 500 µL). Plates were incubated for 3 h in a humid atmosphere of 37 °C with 5% CO_2. Intracellular formazan products were lysed by the addition of 250 µL 10% sodium dodecyl sulfate, and incubation was carried out overnight at room temperature in the dark. Finally, the lysate of each well was homogenized and centrifuged at 10,000 g for 10 min in order to eliminate DEP. The absorbance of each supernatant was recorded at 550 nm using a plate reader (iMark Microplate Absorbance Reader; Bio-Rad, Hercules, CA). The results were expressed as percentage of increase over control cells.

2.11. Chemicals

Fetal bovine serum was obtained from Internegocios (Mercedes, Buenos Aires, Argentina). 2′, 7′-dichlorofluorescein diacetate was provided by Molecular Probes (Eugene, OR, U.S.A), the ELISA kits for TNF-α, IL-1β, IL-6, and IL-8 were purchased from BD Biosciences, Franklin Lakes, NJ. All other chemicals were purchased from Sigma Chemicals (St Louis, MO, U.S.A.).

2.12. Statistical analysis

Statistical calculations were performed using GraphPad PRISM software (San Diego, CA, USA). Data were expressed as mean ± standard error of mean (SEM) and represent the mean of at least 3 independent experiments. The statistical significance of the differences between the two groups of each time point was calculated by unpaired Student's *t*-test, α = 0.05.

3. Results

3.1. Measurement of intracellular ROS generation and sources

3.1.1. Total levels of prooxidant species

Total ROS production was determined by flow cytometry using a DCF-DA probe. Once de-esterified inside de cell, this probe is readily oxidized by oxidant species to a green-fluorescent product DCF. Quantification of MFI showed that the incubation with DEP at 100 µg/mL generated a significant increase in DCF oxidation at all time points evaluated (1 h: 91%; 3 h: 46%; 24 h: 45%, $p < 0.01$), indicating that there is an increased production of intracellular ROS (Fig. 1, A). Fig. 1, B displayed representative overlaid histograms, showing an increase in

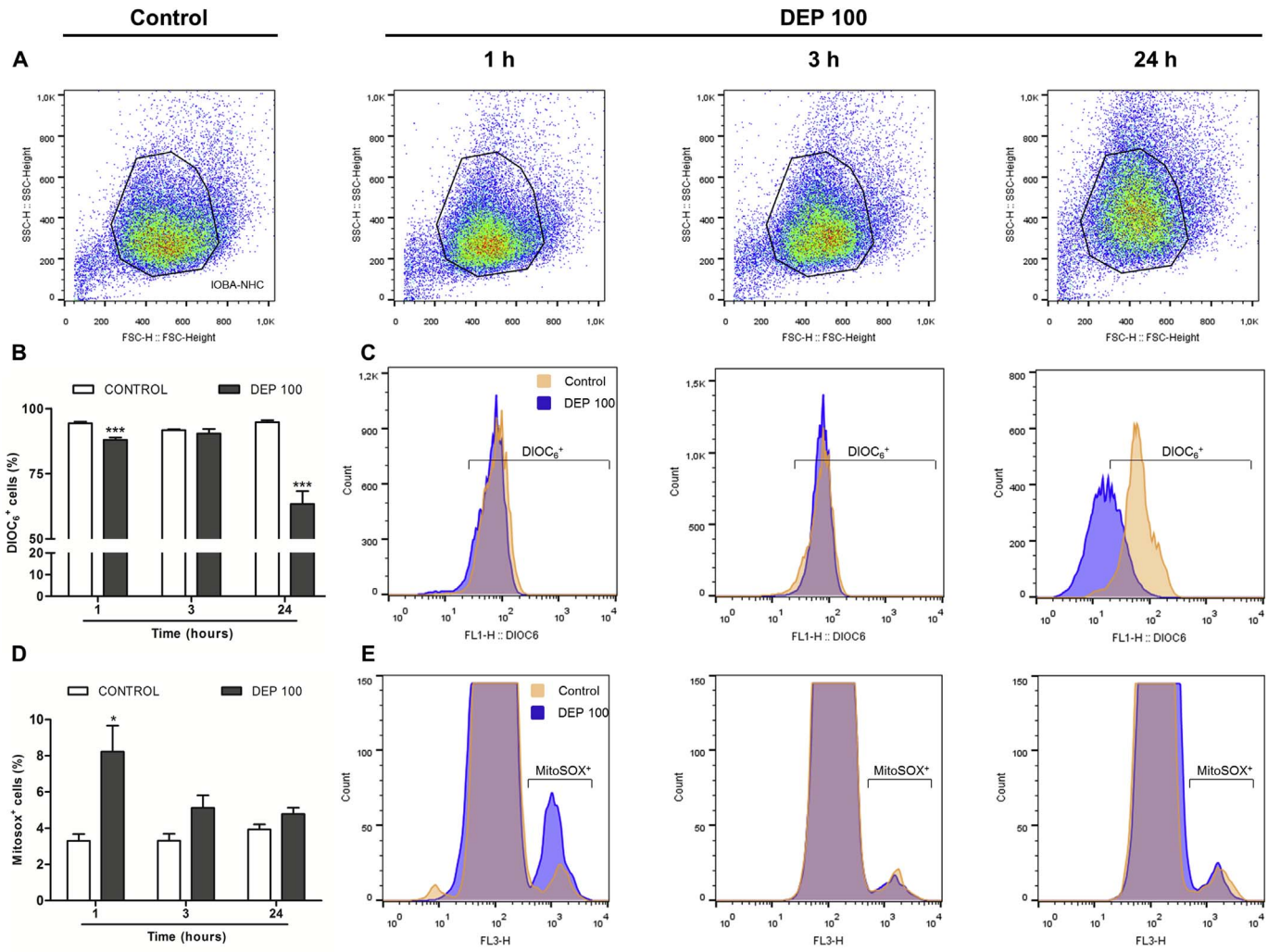

Fig. 3. Inner mitochondrial membrane potential ($\Delta\Psi_m$) and superoxide anion production were determined by Flow Cytometry. A- Cells were selected based on light-scattering properties (SSC vs FSC) and 30,000 events per sample were acquired. B- $DIOC_6$ fluorescence intensity was quantified as MFI in FL-1 channel. Results are expressed as percentage of positive cells ($DIOC_6^+$). C- Representative overlaid histograms of $DIOC_6$ fluorescence of control and DEP 100 groups after 1, 3 and 24 h of exposure. D- MitoSOX fluorescence intensity was quantified as MFI in FL-3 channel. Results are expressed as percentage of positive cells ($MitoSOX^+$). E- Representative overlaid histograms of MitoSOX fluorescence of control and DEP100 groups after 1, 3 and 24 h of exposure. Results are expressed as mean ± SEM. *$p < 0.05$ ***$p < 0.001$.

Table 1
Oxidative damage to macromolecules.[a]

	Time (hour)					
	1		3		24	
	Control	DEP 100	Control	DEP 100	Control	DEP 100
TBARS (nmol MDA/mg protein)	0.90 ± 0.08	1.61 ± 0.13**	1.11 ± 0.12	1.32 ± 0.21	1.13 ± 0.18	0.90 ± 0.09
Carbonyl groups (nmol/mg protein)	10.0 ± 0.7	12.3 ± 1.7	9.8 ± 0.6	13.9 ± 1.5*	8.9 ± 1.0	13.0 ± 0.6*

[a] Values are expressed as mean ± SEM. Results are mean values of at least 3 independent experiments. *$p < 0.05$, **$p < 0.01$.

the signal of FL-1 DCF channel in DEP100 group compared to the control group.

3.1.2. NADPH oxidase-4 (NOX4) expression

NOX4 expression was measured as one of the main sources of intracellular ROS generation. As shown in Fig. 2, an increase in this enzyme expression was found after 3 and 24 h of incubation with DEP compared to the control group (3 h: 61%; 24 h: 47%, $p < 0.05$), indicating that NOX4 contributes to the pro oxidant environment after DEP exposure.

3.1.3. Inner mitochondrial membrane potential ($\Delta\Psi_m$) and superoxide anion production

Mitochondria functionality is vital to cell survival. Mitochondrial membrane potential as well as superoxide anion production are two important function parameters of this organelle. Cells were selected based on light-scattering properties (SSC vs FSC) and 30,000 events per sample were acquired (Fig. 3, A). As exhibited in overlaid $DiOC_6$ fluorescence histograms and quantification of the MFI (Fig. 3B and C), $\Delta\Psi_m$ was lower in DEP 100 group comparing to control group after 1

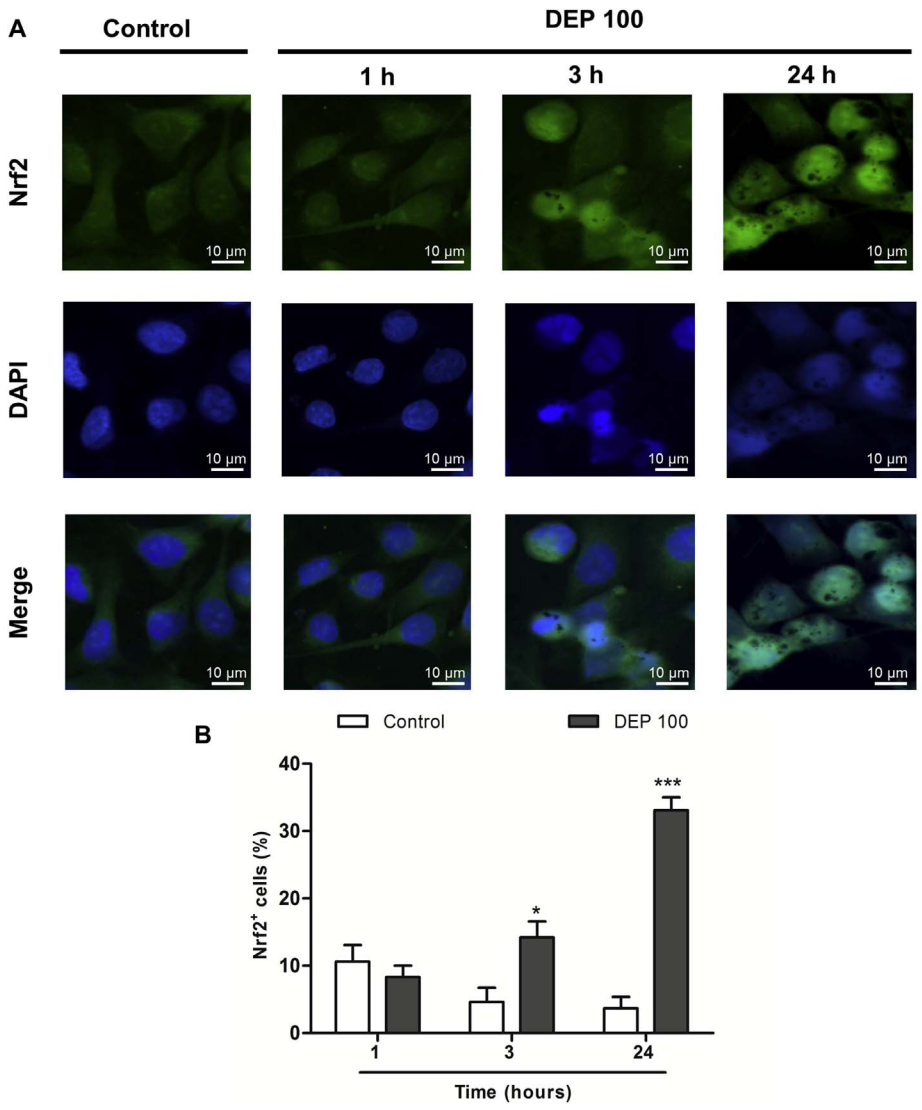

Fig. 4. Nuclear factor-erythroid 2-related factor-2 (Nrf2) immunofluorescence. A- Representative images of fluorescence microscopy of control and DEP100 groups after 1, 3, and 24 h (original magnification 60X). Nrf2 was probed with a primary anti-Nrf2 antibody and visualized with a FITC-conjugated secondary antibody. Nuclei were stained with DAPI. The overlay of blue and green colors in nucleus was considered to be positive for translocation. B- Quantification of cells with Nrf2 nuclear translocation in control and DEP100 groups. Results are expressed as percentage of cells with Nrf2 nuclear translocation ($Nrf2^+$ cells) (mean ± SEM). $*p < 0.05$ $***p < 0.001$. (For interpretation of the references to color in this figure legend, the reader is referred to the Web version of this article.)

and 24 h (7% and 33%, $p < 0.001$). This situation indicates that a significant depolarization of mitochondria membrane takes place when IOBA-NHC are exposed to DEP. An increased production of mitochondria superoxide anion was observed in DEP100 comparing to the control group after 1 h (122%, $p < 0.05$), as it is presented in overlaid histograms and quantification of MFI of $MitoSOX^+$ cells (Fig. 3D and E). No significant difference was observed after 3 and 24 h between DEP100 and control groups.

3.2. Oxidative damage to macromolecules

TBARS assay is one of the most commonly used methods for the evaluation of oxidative damage to lipids. TBARS levels were found increased in DEP100 groups after a 1-h-incubation (79%, $p < 0.05$), but there was no significant difference after a 3 or 24 h of incubation comparing to the control group (Table 1). The carbonyl groups of oxidative modified proteins are used as an oxidative stress marker of protein damage. The carbonyl content was significantly increased by 48% and 57% ($p < 0.05$) in DEP100 group after 3 and 24 h. There was no significant difference between the groups after a 1-h-incubation with DEP (Table 1).

3.3. Nuclear factor-erythroid 2-related factor-2 (Nrf2) immunofluorescence

Nuclear translocation of Nrf2 induces the transcription of several genes related to the cell antioxidant response to stress conditions. As shown in Fig. 4, A immunofluorescence assay reveled that Nrf2 was located inside the nuclei in cells exposed to DEP after 3 and 24 h, but remained in the cytosol in control cells. These results suggest that DEP activates Nrf2 by inducing its translocation to the nucleus. After 1 h both groups presented no nuclear translocation. Quantification of cells with Nrf2 nuclear translocation ($Nrf2^+$ cells) showed that there was an increase of 207% and 802% after 3 and 24 h, respectively, $p < 0.05$.

3.4. Activity of antioxidant enzymes defenses and enzymes related to the regulation of the redox status

SOD and GPx are known as primary antioxidant enzymes, as they directly interact with ROS. Both enzymes were found increased at all time points evaluated ($p < 0.05$), as it is shown in Fig. 5A and B. The activity of GST also showed an increase at all time points (1 h: 121%; 3 h: 23%; 24: 45%, $p < 0.05$), indicating a continuous detoxification of DEP over time (Fig. 5, C). The recycling of GSSG to GSH is performed principally by GR, and when GR is not available, TRxR takes place. A significant increment in GR activity was observed in DEP100 group after a 1-h-incubation (46%, $p < 0.01$), meanwhile a significant

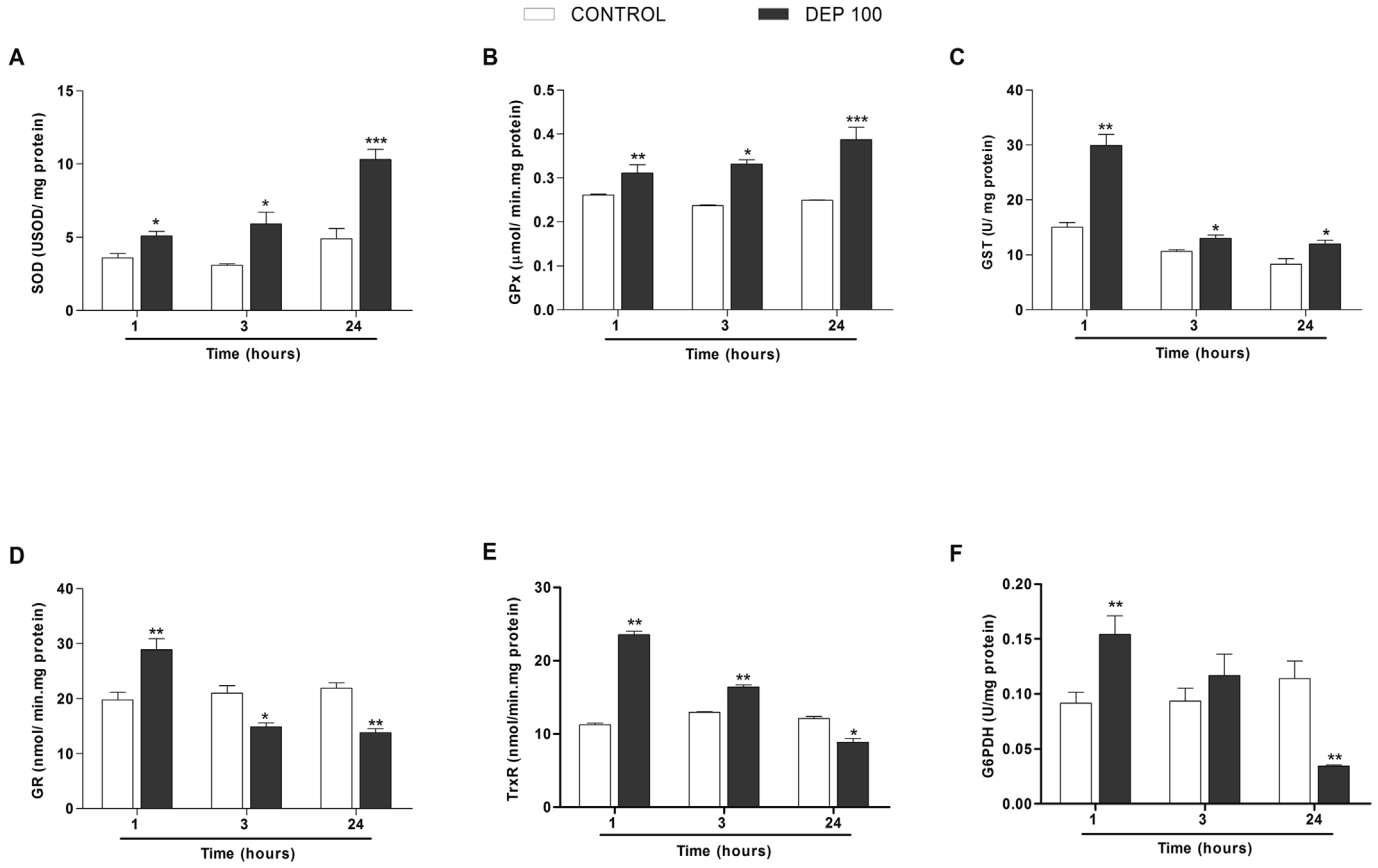

Fig. 5. Activity of antioxidant enzymes defenses and enzymes related to the regulation of the redox status. The activities of the following enzymes were measured in control and DEP100 groups after 1, 3, and 24 h of incubation: A-superoxide dismutase (SOD); B- Glutathione persoxidase (GPx); C- Glutathione S-transferase (GST); D- Gluathione reductase (GR); E-Thioredoxin reductase (TrxR); F: Glucose 6P-dehidrogenase (G6PDH). Results are expressed as mean ± SEM. *$p < 0.05$ **$p < 0.01$ ***$p < 0.001$.

decrease in its activity was found after 3 and 24 h (29% and 37%, respectively, $p < 0.05$) (Fig. 5, D). Furthermore, DEP100 group displayed a significant increase of TRxR activity after 1 h and 3 h of incubation (108% and 27%, respectively, $p < 0.01$), but it showed a lower activity after 24 h (38%, $p < 0.05$) (Fig. 5, E). In addition, G6PDH activity contributes to the maintenance of redox status since is the limit step in the synthesis of NADPH. A significant increase in G6PDH activity was observed after a 1-h-incubation with DEP (68%, $p < 0.05$), while a significant decrease was detected after a 24-h-incubation (70%, $p < 0.01$) (Fig. 5, F).

3.5. Glutathione synthesis

3.5.1. Reduced (GSH) glutathione levels

GSH is the most abundant low molecular weight antioxidant, which is determinant for the maintenance of the redox balance. Under these experimental conditions, GSH levels increased in DEP100 groups after 1 and 3 h of incubation (25% and 41%, respectively, $p < 0.05$) comparing to the control group. However, after a 24-h-incubation a decrease in GSH levels was observed (40%, $p < 0.01$) (Fig. 6, A).

3.5.2. Glutamate cysteine ligase (GCL) expression

The level of GCL is considered one of the steps that limit the rate of GSH synthesis. When IOBA-NHC were exposed to DEP, an increase in GCL expression was observed after a 3-h-incubation with the particles (57%, $p < 0.05$). After a 24-h-incubation, GCL expression in DEP100 group was lower (27%, $p < 0.05$) when compared to the control group (Fig. 6, B).

3.5.3. Aminoacid analysis

Cysteine (Cys) and glutamate (Glu) are two important aminoacids needed for the synthesis of glutathione inside the cell. DEP100 group showed a significant increase in both Cys and Glu after 1 h of incubation (Cys: 19% and Glu: 19%, $p < 0.05$), but there were no significant differences for both aminoacids after a 3-h-incubation. After a 24-h-incubation, Cys levels were found increased (27%, $p < 0.01$), but a decrease in Glu concentration was observed (31%, $p < 0.01$) (Fig. 6, C).

3.6. Proinflammatory cytokine determination

Inflammatory mediators were analyzed in IOBA-NHC cells exposed to DEP. DEP100 group presented an increase in IL-6 release after a 3 and 24 h of incubation (70% and 26%, respectively, $p < 0.05$), but there was no release of this cytokine after a 1-h-incubation (Fig. 7, A). IL-8 release showed a different pattern: there was a significant decrease in DEP100 group at all time points evaluated (1 and 3 h: 35%; 24 h: 42%, $p < 0.05$) (Fig. 7, B). The 24 h results are in accordance with the ones reported by Tau et al. (2013). Levels of TNF-α and IL-1β were not detected in these experimental conditions.

3.7. Proliferation

MTT assay revealed an increase in cellular proliferation in DEP100 group after 1 (19%, $p < 0.05$) and 3 h of incubation with DEP (30%, $p < 0.05$). After a 24-h-incubation a decrease in cell proliferation was found in DEP100 group (41%, $p < 0.001$), as it was previously described by Tau et al. (2013) (Fig. 8).

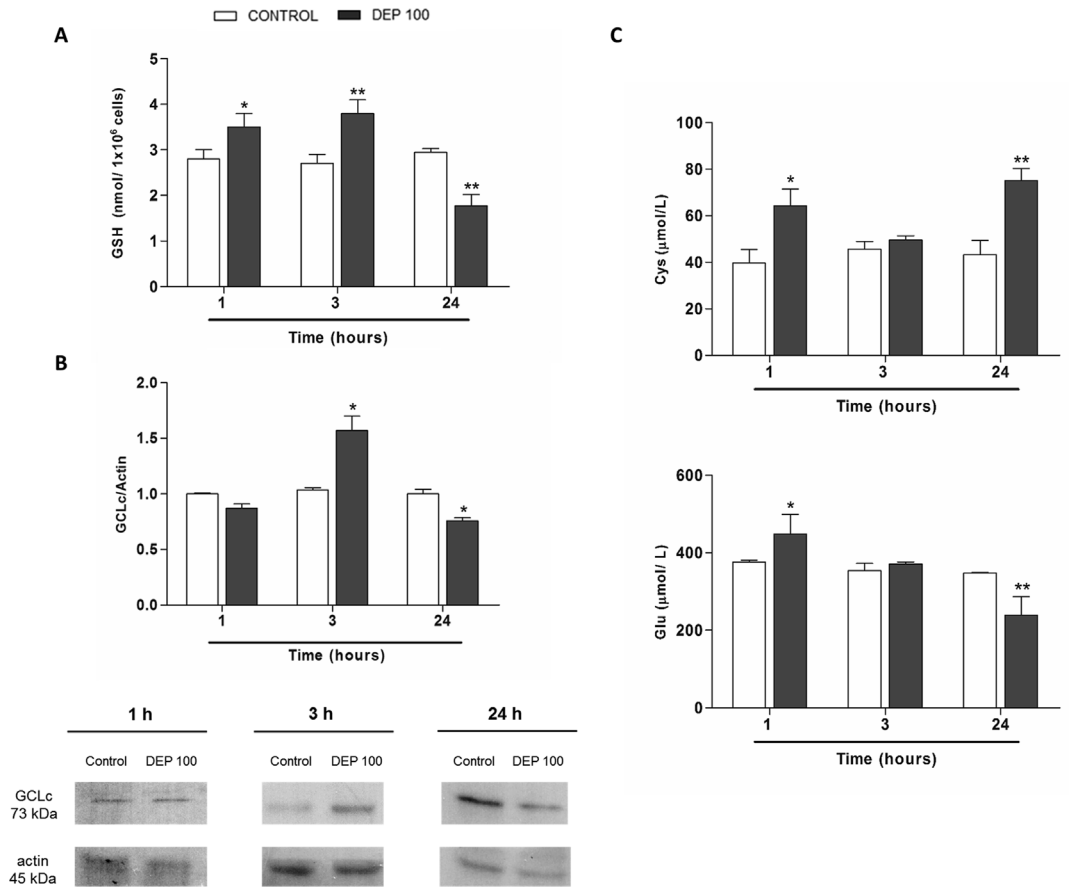

Fig. 6. Glutathione synthesis evaluation. A- GSH levels of control and DEP 100 group after 1, 3, and 24 h. B- Western blotting of GCL expression. A representative blot is shown. Bands of approximately 73 kDa and 45 kDa correspond to GCL and actin, respectively. Bars represent the relative protein level calculated by the ratio of GCL/Actin. C- Amino acids quantification. Cys and Glu levels were assayed in control and DEP100 group after 1, 3, and 24 h. Results are expressed as mean ± SEM. $*p < 0.05$ $**p < 0.01$.

4. Discussion

Clean air is a basic requirement for human health and well-being. Diesel exhaust particles (DEP) are considered to be a central concern regarding the risk to health posed by pollutants from urban air (Wichmann, 2007).

Our work is centered on the evaluation of oxidative stress and inflammatory mediators on the ocular surface due to air pollution, in particularly, the toxic effects of DEP exposure on human conjunctival epithelial cells. The ocular surface is constantly exposed to the environment: radiation, atmospheric oxygen, and air pollutants. In this work, we found that there is a persistent increase over time of ROS, reaching a maximum level after 1 h of incubation with DEP. The generation of ROS is thought to contribute to ocular surface damage. There are mainly two different sources of ROS, mitochondria and NADPH-oxidases. In this model, we have identified these two sources, which change over the exposure time. After 1 h of exposure, it appears that mitochondrial is alters since the increased production of superoxide anion takes place. It has been demonstrated that the organic chemical compounds adsorbed to DEP are capable to generate mitochondria injury and to increase ROS production (Li et al., 2008; Park et al., 2011; Vattanasit et al., 2014). After 3 and 24 h superoxide anion levels presented no significant differences. This situation could be explained by the increase in SOD activity, which seems to be capable of removing the superoxide anion produced by the mitochondria. Moreover, the inner membrane potential was affected since the first hour, reaching a minimum level after 24 h. It has been reported that mitochondria depolarization could also lead to the release of apoptogenic factors and loss of oxidative phosphorylation altering ATP production (Ly et al., 2003). The induction of NADPH oxidases has been identified as another source of ROS triggered by particulate matter in other tissues (Kampfrath et al., 2011; Lee et al., 2016; Magnani et al., 2013). In this work, the induction of NOX4 was observed since the third hour of incubation with DEP. This event appears later than the mitochondrial response, when the cell also undergoes a proinflammatory response mediated by IL-6. In accordance, several works have shown that there is a link between both IL-6 and NADPH oxidases induction, in which IL-6 promotes NADPH oxidase expression and vice versa (Behrens et al., 2008; Didion, 2017; Park et al., 2006; Yu et al., 2005).

ROS are highly reactive molecules that interact with several biological targets in the cell, such as carbohydrates, nucleic acids, lipids, and proteins, altering their functions (Birben et al., 2012). In this model, the maximum in ROS production concurs with the lipid damage detected after a 1-h-incubation with DEP, suggesting that lipids could be the earliest molecular targets of oxidative damage, since after 3 h of incubation lipid peroxidation levels returned to control values. GPx removes lipid hydroperoxides from lipid peroxidation process. Therefore, an increase in GPx activity could result in the removal of lipid chain reaction intermediaries, preventing the propagation step (Imai and Nakagawa, 2003). TRxR is another alternative pathway for the detoxification of hydroperoxides, which in conjunction with GPx may be responsible for the return to control values of lipid peroxidation markers. In contrast, protein carbonylation seems to be a late event, since protein damage was detected after 3 h of incubation with DEP, and persisted after a 24-h-incubation. The accumulation of protein carbonyls over time is consisted with the fact that carbonylated proteins can not be repaired by cellular enzymes (Fedorova et al., 2014).

In this context, a well-established antioxidant defense system is important in order to maintain the redox balance and to avoid cell oxidative damage (Halliwell and Gutteridge, 2006). The enhancing of

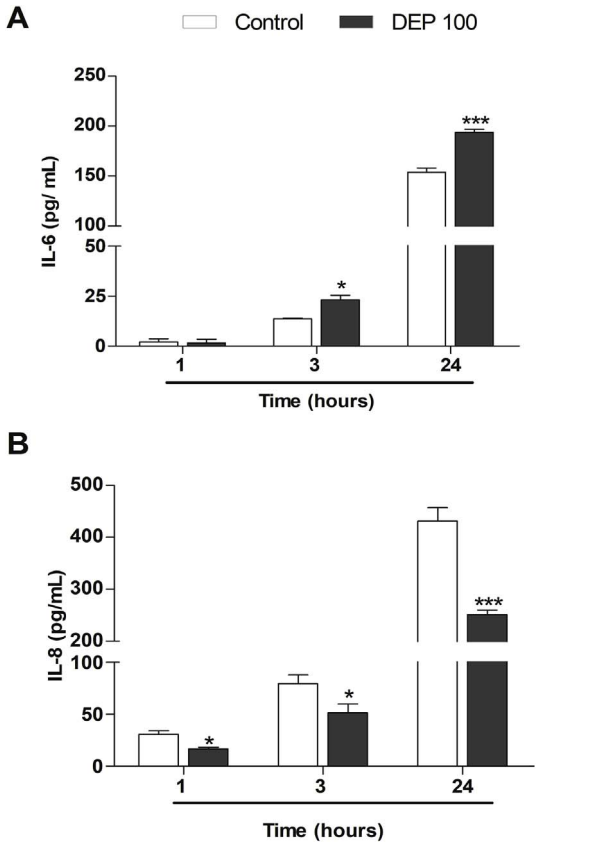

Fig. 7. Proinflammatory cytokine determination. IL-6 (A) and IL-8 (B) levels in control and DEP100 groups after 1, 3, and 24 h of incubation with DEP. Results are expressed as mean ± SEM. *$p < 0.05$.

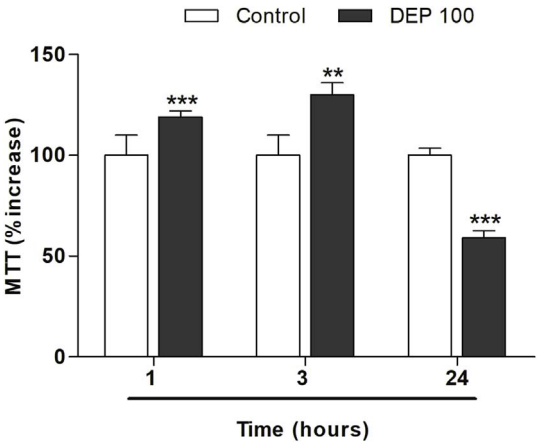

Fig. 8. Proliferation measured by MTT assay of control and DEP100 groups after 1,3, and 24 h. Results are expressed as fold of increase. Results are expressed as mean ± SEM. *$p < 0.05$ **$p < 0.01$ ***$p < 0.001$.

cellular antioxidant capacity is mainly provided by the activation of Nrf2 signaling pathway. It has been shown that Nrf2 is an important factor in the prevention of the allergic airway inflammatory response and the oxidative stress induced by DEP (Li et al., 2013). To our knowledge, this is the first time that Nrf2 involvement is described as a conjunctiva response to particulate matter. In this work, we demonstrated that DEP-induced redox imbalance triggered the activation of Nrf2 in human conjunctival epithelial cells, as a strategy for increasing cellular antioxidant capacity. Our findings are in accordance with the fact that it takes close to 2 h from the time of exposure to optimally switch on nuclear import of Nrf2 (Jain et al., 2005). Therefore, Nrf2 seems to be essential in the development of the cellular response to DEP since the third hour of exposure. Furthermore, we found an increase in the activity of all antioxidant enzymes evaluated on conjunctival epithelial cells after 1 h of incubation with DEP, suggesting an early adaptive response to the increased production of oxidant species. G6PDH contributes to the antioxidant defenses of the cell by maintaining the cellular reductive potential in the form of NADPH through the pentose phosphate pathway. Thus, an increment of its activity indicates that there is a concomitant increase in the synthesis of NADPH, which is needed as a cofactor by several antioxidant enzymes such as GPx, GR and TRxR. After 24 h, Nrf2 activation is still enhanced but the cellular antioxidant capacity provided by this pathway is exceeded. This situation results in increased ROS production and oxidative damage to proteins. Further studies would be needed in order to identify the specific set of downstream genes that Nrf2 nuclear translocation activates under these experimental conditions.

GSH is essential to maintain the intracellular redox balance and for several cellular processes such as redox signaling, detoxification of xenobiotics, regulation of cell proliferation, apoptosis, immune function, and fibrogenesis (Lu, 2009; Lu, 2014a,b). The balance between the reduced and the oxidized form, GSH and GSSG, respectively, mainly results from three factors: GSH consumption, GSSG/GSH recycling and GSH synthesis. First, GSH could act as a cofactor of antioxidant and detoxifying enzymes such as GPx and GST. So the increase in the activity of those enzymes leads to the increased consumption of GSH, generating GSSG. This situation could be corrected by the action of the enzymes that could recycle GSH from its oxidized form: GR and TrxR. Both are two key enzymes in the recycling of the majors sulfhydryl groups donators, GSH and thioredoxin, respectively, which contribute to the maintenance of redox balance. TRxR could also play an important role in the GSSG/GSH recycling since it has been shown that thioredoxin could efficiently reduce GSSG to GSH when GR is not available (Nordberg and Arnér, 2001). Finally, the synthesis of GSH, tripeptide composed of γ-L-glutamyl-L-cysteinyl-glycine, is determined by two factors: cysteine availability and glutamate cysteine ligase (GCL) activity, which is considered the rate limiting step.

In this experimental model, intracellular GSH levels were found increased after 1 and 3 h of incubation with DEP, despite the increase in its consumption due to the enhanced activity of the antioxidant enzymes. The increment in GR activity as well as a greater availability of cysteine and glutamate after the first hour of incubation with DEP would enhance both the GSSG recycling and the *de novo* synthesis of GSH, respectively. After the third hour of exposure to DEP, GSH levels are also incremented, not at the expense of GR activity but due to the induction of GCL expression. Although the concentration of cysteine is almost the same as the control value, the *de novo* synthesis still plays an important role since another crucial function of GSH is the storage of cysteine. High levels of cysteine could be dangerous for cells because it is unstable and rapidly auto-oxidizes to cystine, producing oxygen free radicals in the process (Meister, 1988). After a 24 h exposure, GSH levels are depleted and this situation could be due to an increase in its consumption as well as a decrease in GSSG/GSH recycling and the impaired GSH synthesis. The decrease in GR and GCL as wells as the still enhanced activity of GPx and GST after a 24-h-incubation with DEP support this hypothesis.

In the present work, we have established a time course of oxidative stress and inflammatory markers: the results suggest that ROS production seem to be an earlier event triggered by the exposure of human conjunctival epithelial cells to DEP, in comparison to the proinflammatory response mediated by IL-6. We found no release of TNF-α or IL-1β, suggesting that these cytokines are not implicated in the toxic mechanism triggered by DEP on IOBA-NHC. Also, we detected a significant decrease of IL-8 at all time points evaluated. It has been established that phase II enzymes induction could protect the cell from the proinflammatory effects of DEP mediated by IL-8 (Ritz et al., 2007), and in this study all these enzymes are overstimulated since the first

hour of incubation with DEP. We also found that DEP stimulate cellular proliferation after short exposures, indicating that cellular hyperplasia could be an adaptive change of the epithelia to particulate matter, as it has been demonstrated in epithelial lung cells incubated with DEP (Bayram et al., 2006). Despite the fact that under short periods of exposure to DEP lipids and then proteins are targets of oxidative damage, the extent of that damage is not affecting the viability of human conjunctival epithelial cells at early time points. This situation suggests that the antioxidant mechanisms mediated by Nrf2 pathway under short periods of exposure to DEP as well as the cell hyperplasia are successful in avoiding cell death. However, after a 24-h-incubation with DEP the scenario is quite different: the epithelial cell capacity to maintain redox balance is exceeded as a result of cumulative oxidative stress. This situation could be aggravated by the maximum reached in IL-6 release which provides an untoward proinflammatory situation. NADPH oxidase-4 activity as well as mitochondria depolarization contribute to the redox status imbalance, as levels of GSH and antioxidant enzyme response are not enough to counteract the increased ROS production. Under these conditions, significant increase of oxidative damage and apoptosis take place (Tau et al., 2013; Lasagni Vitar et al., 2015). In the recent years, it has been proposed that the depletion of intracellular GSH is involved in the activation of several apoptotic signaling pathways (Circu and Aw, 2012; Marí et al., 2009). Therefore, the cellular GSH pool could be essential in cell survival after the exposure to DEP.

The continuous exposure to air particulate matter would affect the conjunctival epithelia integrity, increasing the susceptibility to ocular surface affections. The findings of this work would be useful for the better understanding of ocular symptoms manifested by people living in urban centers due to the exposure to air particulate matter. This is the first time that a time course of oxidative stress and inflammatory markers due to DEP exposure has been studied on human conjunctiva epithelial cells, involving mitochondria and NADPH oxidase activation, as well as the Nrf2 pathway to develop the cellular antioxidant response to air pollutants.

5. Conclusions

In this work, we demonstrate that the response of human conjunctival epithelial cells to DEP differs through the exposure time. DEP induces an early redox imbalance followed by an IL-6 mediated inflammatory response. At first, the oxidative environment generated principally by mitochondrial superoxide anion produce a cellular adaptive response consisted of an increase of both enzymatic and non-enzymatic antioxidants. After 3 h, NADPH oxidase-4 is presented as main source of ROS, when the cell also starts to experiment a proinflammatory response mediated by IL-6. At this time point, the nucleus translocation of Nrf2 is stimulated, attempting to enhance the cellular antioxidant capacity. Although after 24 h Nrf2 pathway is still enhanced, the epithelial cell capacity to maintain redox balance is exceeded, as the antioxidant enzymes activation and the depleted GSH pool are not capable of counteracting the increased ROS production. Under these conditions, and taking into account our results, conjunctival epithelial cell injury by air pollutants may be relevant on people living in urban centers that show eye discomfort symptoms.

Financial support

This work was supported by grants 01/796BA from University of Buenos Aires, Argentina and Prest.BID.PICT2012-0328 from Agencia Nacional de Promoción Científica y Tecnológica (ANPCyT), Argentina.

Disclosure/conflict of interest

The Authors do not have any conflicts of interest to declare.

Acknowledgements

The authors want to thank to María Isabel Giménez, Ph. D. and Ignacio Bressan, MS for the helpful assistance in the aminoacid evaluation (Departamento de Bioquímica Aplicada, Área Espectometría de Masa, Instituto Universitario, Hospital Italiano). The authors are grateful to Timoteo Marchini, Ph. D. and Pablo Evelson, Ph. D. for the helpful assistance on the Flow Cytometry experiments and analysis.

Appendix A. Supplementary data

Supplementary data related to this article can be found at http://dx.doi.org/10.1016/j.exer.2018.03.005.

References

Bayram, H., Ito, K., Issa, R., Ito, M., Sukkar, M., Chung, K.F., 2006. Regulation of human lung epithelial cell numbers by diesel exhaust particles. Eur. Respir. J. 27, 705–713. http://dx.doi.org/10.1183/09031936.06.00012805.

Behrens, M.M., Ali, S.S., Dugan, L.L., 2008. Interleukin-6 mediates the increase in NADPH-oxidase in the ketamine model of schizophrenia. J. Neurosci. 28, 13957–13966. http://dx.doi.org/10.1523/JNEUROSCI.4457-08.2008.

Berra, M., Galperín, G., Dawidowski, L., Tau, J., Márquez, I., Berra, A., 2015. Impact of wildfire smoke in Buenos Aires, Argentina, on ocular surface. Arq. Bras. Oftalmol. 78, 110–114. http://dx.doi.org/10.5935/0004-2749.20150028.

Birben, E., Murat, U., Md, S., Sackesen, C., Erzurum, S., Kalayci, O., 2012. Oxidative stress and antioxidant defense. WAO J. 5, 9–19. http://dx.doi.org/10.1097/WOX.0b013e3182439613.

Chen, Y., Mehta, G., Vasiliou, V., 2009. Antioxidant defences in the ocular surface. Ocul. Surf. 18, 1199–1216. http://dx.doi.org/10.1016/j.micinf.2011.07.011.Innate.

Circu, M.L., Aw, T.Y., 2012. Glutathione and modulation of cell apoptosis. Biochim. Biophys. Acta Mol. Cell Res. 1823, 1767–1777. http://dx.doi.org/10.1016/j.bbamcr.2012.06.019.

Didion, S., 2017. Cellular and oxidative mechanisms associated with Interleukin-6 signaling in the vasculature. Int. J. Mol. Sci. 18, 2563. http://dx.doi.org/10.3390/ijms18122563.

Diebold, Y., Calonge, M., Enríquez de Salamanca, A., de Salamanca, A.E., Callejo, S., Corrales, R.M., Sáez, V., Siemasko, K.F., Stern, M.E., 2003. Characterization of a spontaneously immortalized cell line (IOBA-NHC) from normal human conjunctiva. Invest. Ophthalmol. Vis. Sci. 44, 4263–4274.

Fedorova, M., Bollineni, R.C., Hoffmann, R., 2014. Protein carbonylation as a major hallmark of oxidative damage: update of analytical strategies. Mass Spectrom. Rev. 33, 79–97. http://dx.doi.org/10.1002/mas.21381.

Flohé, L., Günzler, W.A., 1984. Assays of glutathione peroxidase. Methods Enzymol. 105, 114–121.

Fu, Q., Mo, Z., Lyu, D., Zhang, L., Qin, Z., Tang, Q., Yin, H., Xu, P., Wu, L., Lou, X., Chen, Z., Yao, K., 2017. Air pollution and outpatient visits for conjunctivitis: a case-crossover study in Hangzhou, China. Environ. Pollut. 231, 1344–1350. http://dx.doi.org/10.1016/j.envpol.2017.08.109.

Habig, W.H., Pabst, M.J., Jakoby, W.B., 1974. Glutathione S-transferases. The first enzymatic step in mercapturic acid formation. J. Biol. Chem. 249, 7130–7139.

Halliwell, B., Gutteridge, J.M.C., 2006. Free Radicals in Biology and Medicine, fourth ed. (Oxford).

Holmgren, A., Björnstedt, M., 1995. Thioredoxin and thioredoxin reductase. Methods Enzymol. 252, 199–208.

Hwang, S.H., Choi, Y.-H., Paik, H.J., Wee, W.R., Kim, M.K., Kim, D.H., 2016. Potential importance of ozone in the association between outdoor air pollution and dry eye disease in South Korea. JAMA Ophthalmol. 134, 503. http://dx.doi.org/10.1001/jamaophthalmol.2016.0139.

Imai, H., Nakagawa, Y., 2003. Biological significance of phospholipid hydroperoxide glutathione peroxidase (PHGPx, GPx4) in mammalian cells. Free Radic. Biol. Med. 34, 145–169. http://dx.doi.org/10.1016/S0891-5849(02)01197-8.

Jain, A.K., Bloom, D.A., Jaiswal, A.K., 2005. Nuclear import and export signals in control of Nrf2. J. Biol. Chem. 280, 29158–29168. http://dx.doi.org/10.1074/jbc.M502083200.

Kampfrath, T., Maiseyeu, A., Ying, Z., Shah, Z., Deiuliis, J.A., Xu, X., Kherada, N., Brook, R.D., Reddy, K.M., Padture, N.P., Parthasarathy, S., Chen, L.C., Moffatt-Bruce, S., Sun, Q., Morawietz, H., Rajagopalan, S., 2011. Chronic fine particulate matter exposure induces systemic vascular dysfunction via NADPH oxidase and TLR4 pathways. Circ. Res. 108, 716–726. http://dx.doi.org/10.1161/CIRCRESAHA.110.237560.

Laks, D., de Oliveira, R.C., de André, P.A., Macchione, M., Lemos, M., Faffe, D., Saldiva, P.H.N., Zin, W.A., 2008. Composition of diesel particles influences acute pulmonary toxicity: an experimental study in mice. Inhal. Toxicol. 20, 1037–1042. http://dx.doi.org/10.1080/08958370802112922.

Lasagni Vitar, R.M., Tau, J., Reides, C.G., Berra, A., Ferreira, S.M., Llesuy, S.F., 2015. Evaluation of oxidative stress markers in human conjunctival epithelial cells exposed to diesel exhaust particles (DEP). Invest. Ophthalmol. Vis. Sci. 56, 7058–7066. http://dx.doi.org/10.1167/iovs.15-16864.

Lee, C.-W., Lin, Z.-C., Hu, S.C.-S., Chiang, Y.-C., Hsu, L.-F., Lin, Y.-C., Lee, I.-T., Tsai, M.-H., Fang, J.-Y., 2016. Urban particulate matter down-regulates filaggrin via COX2 expression/PGE2 production leading to skin barrier dysfunction. Sci. Rep. 6http://dx.

doi.org/10.1038/srep27995. 27995.
Lee, I.T., Yang, C.M., 2012. Role of NADPH oxidase/ROS in pro-inflammatory mediators-induced airway and pulmonary diseases. Biochem. Pharmacol. http://dx.doi.org/10.1016/j.bcp.2012.05.005.
Leong, S.F., Clark, J.B., 1984. Regional enzyme development in rat brain. Enzymes of energy metabolism. Biochem. J. 218, 139–145.
Levine, R.L., Garland, D., Oliver, C.N., Amici, A., Climent, I., Lenz, A.G., Ahn, B.W., Shaltiel, S., Stadtman, E.R., 1990. Determination of carbonyl content in oxidatively modified proteins. Methods Enzymol. 186, 464–478.
Li, N., Xia, T., Nel, A.E., 2008. The role of oxidative stress in ambient particulate matter-induced lung diseases and its implications in the toxicity of engineered nanoparticles. Free Radic. Biol. Med. http://dx.doi.org/10.1016/j.freeradbiomed.2008.01.028.
Li, Y.J., Kawada, T., Azuma, A., 2013. Nrf2 is a protective factor against oxidative stresses induced by diesel exhaust particle in allergic asthma. Oxid. Med. Cell. Longev. 2013. http://dx.doi.org/10.1155/2013/323607.
Lu, S.C., 2009. Regulation of glutathione synthesis. Mol. Aspect. Med. 30, 42–59. http://dx.doi.org/10.1016/j.mam.2008.05.005.REGULATION.
Lu, Shelly C., 2014a. Comparative quantification of health risks global and regional burden of disease attributable to selected major risk factors. Biochim. Biophys. Acta. http://dx.doi.org/10.1016/j.bbagen.2012.09.008.GLUTATHIONE.
Lu, Shelly C., 2014b. Glutathione synthesis. Biochim. Biophys. Acta 1830, 3143–3153. http://dx.doi.org/10.1016/j.bbagen.2012.09.008.GLUTATHIONE.
Ly, J.D., Grubb, D.R., Lawen, A., 2003. The mitochondrial membrane potential (δψm) in apoptosis; an update. Apoptosis. http://dx.doi.org/10.1023/A:1022945107762.
Magnani, N.D., Marchini, T., Tasat, D.R., Alvarez, S., Evelson, P.A., 2011. Lung oxidative metabolism after exposure to ambient particles. Biochem. Biophys. Res. Commun. 412, 667–672. http://dx.doi.org/10.1016/j.bbrc.2011.08.021.
Magnani, N.D., Marchini, T., Vanasco, V., Tasat, D.R., Alvarez, S., Evelson, P., 2013. Reactive oxygen species produced by NADPH oxidase and mitochondrial dysfunction in lung after an acute exposure to Residual Oil Fly Ashes. Toxicol. Appl. Pharmacol. 270, 31–38. http://dx.doi.org/10.1016/j.taap.2013.04.002.
Magnani, N.D., Muresan, X.M., Belmonte, G., Cervellati, F., Sticozzi, C., Pecorelli, A., Miracco, C., Marchini, T., Evelson, P., Valacchi, G., 2016. Skin damage mechanisms related to airborne particulate matter exposure. Toxicol. Sci. 149, 227–236. http://dx.doi.org/10.1093/toxsci/kfv230.
Marchini, T., Magnani, N.D., Paz, M.L., Vanasco, V., Tasat, D., González Maglio, D.H., Alvarez, S., Evelson, P.A., 2014. Time course of systemic oxidative stress and inflammatory response induced by an acute exposure to Residual Oil Fly Ash. Toxicol. Appl. Pharmacol. 274, 274–282. http://dx.doi.org/10.1016/j.taap.2013.11.013.
Marí, M., Morales, A., Colell, A., García-Ruiz, C., Fernández-Checa, J.C., 2009. Mitochondrial glutathione, a key survival antioxidant. Antioxidants Redox Signal. 11, 2685–2700. http://dx.doi.org/10.1089/ars.2009.2695.
Meister, A., 1988. Glutathione metabolism and its selective modification. J. Biol. Chem. 263, 17205–17208.
Misra, H.P., Fridovich, I., 1972. The role of superoxide anion in the autoxidation of epinephrine and a simple assay for superoxide dismutase. J. Biol. Chem. 247, 3170–3175.
Nel, A., 2005. Atmosphere: enhanced: air pollution-related illness: effects of particles. Science 308, 804–806. http://dx.doi.org/10.1126/science.1108752. (80).
Nezzar, H., Mbekeani, J.N., Noblanc, A., Chiambaretta, F., Drevet, J.R., Kocer, A., 2017. Investigation of antioxidant systems in human meibomian gland and conjunctival tissues. Exp. Eye Res. 165, 99–104. http://dx.doi.org/10.1016/j.exer.2017.09.005.
Nordberg, J., Arnér, E.S.J., 2001. Reactive oxygen species, antioxidants, and the mammalian thioredoxin system. Free Radic. Biol. Med. 31, 1287–1312. http://dx.doi.org/10.1016/S0891-5849(01)00724-9.
Nucci, P., Sacchi, M., Pichi, F., Allegri, P., Serafino, M., Dello Strologo, M., De Cillà, S., Villani, E., 2017. Pediatric conjunctivitis and air pollution exposure: a prospective observational study. Semin. Ophthalmol. 32, 407–411. http://dx.doi.org/10.3109/08820538.2015.1115088.
Park, E.-J., Roh, J., Kang, M.-S., Kim, S.N., Kim, Y., Choi, S., 2011. Biological responses to diesel exhaust particles (DEPs) depend on the physicochemical properties of the DEPs. PLoS One 6, e26749. http://dx.doi.org/10.1371/journal.pone.0026749.
Park, H.S., Chun, J.N., Jung, H.Y., Choi, C., Bae, Y.S., 2006. Role of NADPH oxidase 4 in lipopolysaccharide-induced proinflammatory responses by human aortic endothelial cells. Cardiovasc. Res. 72, 447–455. http://dx.doi.org/10.1016/j.cardiores.2006.09.012.
Racker, E., 1955. Glutathione reductase from bakers' yeast and beef liver. J. Biol. Chem. 217, 855–865.
Ritz, S.A., Wan, J., Diaz-Sanchez, D., 2007. Sulforaphane-stimulated phase II enzyme induction inhibits cytokine production by airway epithelial cells stimulated with diesel extract. Am. J. Physiol. Lung Cell Mol. Physiol. 292.
Rubio, V., Valverde, M., Rojas, E., 2010. Effects of atmospheric pollutants on the Nrf2 survival pathway. Environ. Sci. Pollut. Res. 17, 369–382. http://dx.doi.org/10.1007/s11356-009-0140-6.
Tau, J., Novaes, P., Matsuda, M., Tasat, D.R., Saldiva, P.H., Berra, A., 2013. Diesel exhaust particles selectively induce both proinflammatory cytokines and mucin production in cornea and conjunctiva human cell lines. Investig. Opthalmology Vis. Sci. 54, 4759. http://dx.doi.org/10.1167/iovs.12-10541.
Torricelli, A.A.M., Matsuda, M., Novaes, P., Braga, A.L.F., Saldiva, P.H.N., Alves, M.R., Monteiro, M.L.R., 2014. Effects of ambient levels of traffic-derived air pollution on the ocular surface: analysis of symptoms, conjunctival goblet cell count and mucin 5AC gene expression. Environ. Res. 131, 59–63. http://dx.doi.org/10.1016/j.envres.2014.02.014.
Tsubota, K., Tseng, S.C.G., Nordlund, M.L., 2002. Anatomy and Physiology of the Ocular Surface, in: Ocular Surface Disease Medical and Surgical Management. Springer-Verlag, New York, pp. 3–15. http://dx.doi.org/10.1007/0-387-21570-0_1.
Vattanasit, U., Navasumrit, P., Khadka, M.B., Kanitwithayanun, J., Promvijit, J., Autrup, H., Ruchirawat, M., 2014. Oxidative DNA damage and inflammatory responses in cultured human cells and in humans exposed to traffic-related particles. Int. J. Hyg Environ. Health 217, 23–33. http://dx.doi.org/10.1016/j.ijheh.2013.03.002.
Wichmann, H.-E., 2007. Diesel exhaust particles. Inhal. Toxicol. 19 (Suppl. 1), 241–244. http://dx.doi.org/10.1080/08958370701498075.
World Health Organization, 2016. Ambient Air Pollution: a Global Assessment of Exposure and Burden of Disease. World Health Organization doi:9789241511353.
Xia, T., Kovochich, M., Nel, A.E., 2007. Impairment of mitochondrial function by particulate matter (PM) and their toxic components: implications for PM-induced cardiovascular and lung disease. Front. Biosci. 12, 1238–1246 doi:2142 [pii].
Yagi, K., 1976. A simple fluorometric assay for lipoperoxide in blood plasma. Biochem. Med. 15, 212–216.
Yu, J.H., Lim, J.W., Kim, H., Kim, K.H., 2005. NADPH oxidase mediates interleukin-6 expression in cerulein-stimulated pancreatic acinar cells. Int. J. Biochem. Cell Biol. 37, 1458–1469. http://dx.doi.org/10.1016/j.biocel.2005.02.004.